



3D simulation of a giant oilfield in calcareous formations and scrutiny study of the interaction of the calculated parameters (Asmari formation in Maroon oilfield, Iran)

Mazdak Ghasemi Tootkaboni¹ · Nasser Ebadati² · Arman Naderi³

Received: 29 January 2021 / Accepted: 22 April 2021 / Published online: 30 April 2021
© Saudi Society for Geosciences 2021

Abstract

Simulation is an art to model the reservoir's structure in the petroleum industry, which transfers all possible data digitally to the reservoir management system's suitable computation software. The present study attempts to construct a 3D structural model using the geostatistical method to access in situ oil volume and the best oil production position. The geological area is the Maroon oilfields located at Dezful Embayment in southwest of Iran. In this oilfield, the Asmari reservoir is divided into ten zones. Several steps such as gridding, kriging, and experimental variogram were carried out to access all available data to make up the model. The evaluation revealed that zones one and five were the main oil-bearing layers since it contains about 60% of total oil volume in this field. Petrophysical parameter distribution indicated that zones four and seven are good candidates for oil production since they have higher porosity and net to growth thickness than other zones. From the seventh to the tenth zone, the oil volume decreased due to high water saturation in these areas. The best zones for the future program are located in the western part. This study shows that 3D modeling will find elongation-type anticline and reservoir direction and the best location for future drilling programs based on the interaction of the petrographic parameters. The results can be used in various steps during the lifetime of the different reservoirs around the globe.

Keywords Geostatistics · Hydrocarbon · Petrophysical parameters · Petroleum · Reservoir

Introduction

Understanding the subsurface structure is an essential part of any hydrocarbon reservoir-characterization study. Reservoir characterization and modeling obtained by this valuable

information count as important keys for well managing and production in oil fields (Aarnes 2004; Al-Bulushi et al. 2012; Avansi et al. 2016). In recent years, various technologies and new models are applied to understand prospective reservoirs and provide different information types such as geological, petrophysical, geophysical, pressure profiles, and production history (Chen and Durlofsky 2006). Over the last decades, many researchers demonstrated that the new models could determine some essentials, including oil amount in the giant oilfields and optimum drilling locations, introduce undeveloped fields, and have an economic estimate of the projects before they start (Christoforos and Dario 2010; Le Ravalec et al. 2014; Nikraves and Zadeh 2007; Pouladi et al. 2017). The conventional methods, such as classical statistics, are no longer helpful in the vast reservoirs and are obsolete (Zhi and Caineng 2019). Because (i) their estimated petrophysical parameters do not show significant correlations in heterogeneous hydrocarbon reservoirs (Elkatatny et al. 2018), (ii) they are costly and need a large number of core samples and wells (Al-Ajmi and Holditch 2000), and (iii) the modeling takes a

Responsible Editor: Santanu Banerjee

✉ Arman Naderi
naderi.arman@gmail.com

Mazdak Ghasemi Tootkaboni
mazdak.ghasemi@yahoo.com

Nasser Ebadati
drebadati@yahoo.com

¹ Department of Petroleum and Mining Engineering, Central Tehran Branch, Islamic Azad University, Tehran, Iran

² Department of Geology, Islamshahr Branch, Islamic Azad University, Islamshahr, Iran

³ Department of Soil Science, University of Zanjan, Zanjan, Iran

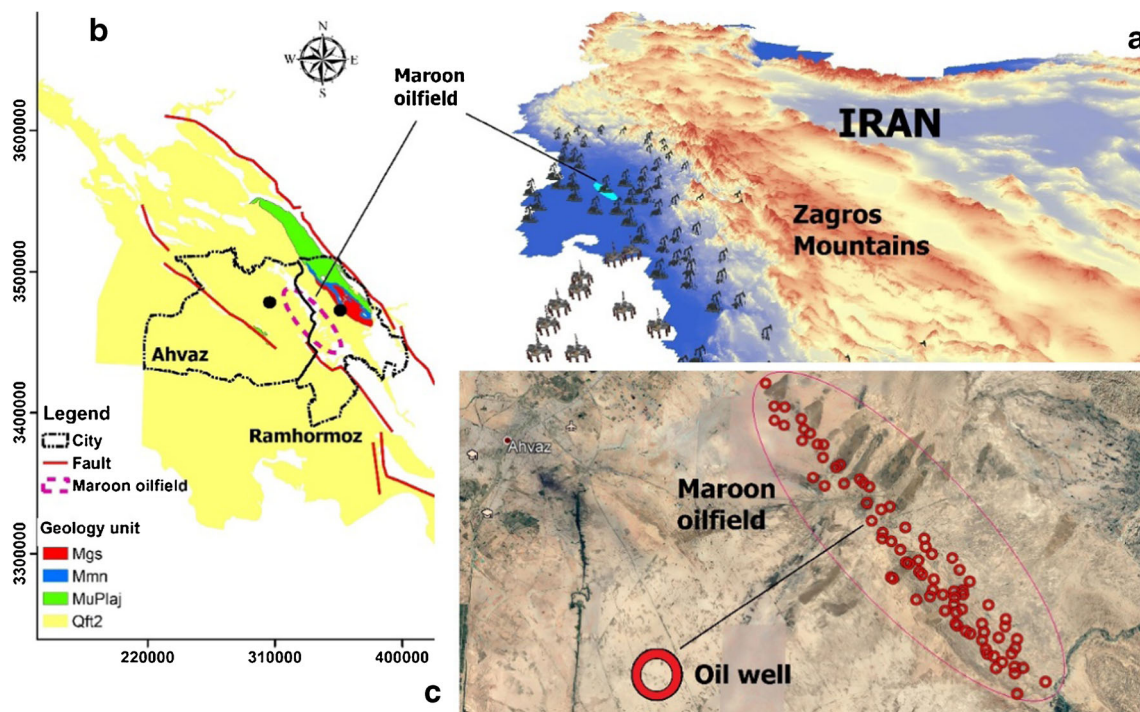


Fig. 1 Geographical position of **a** Zagros oilfields, **b** surface geology in Maroon oilfield, and **c** studied oil wells in Maroon oilfield (Mgs: gray, and red marl alternating with anhydrite, argillaceous limestone, and limestone; Mmn: low weathering gray marls alternating with bands of

more resistant shelly limestone; MuPlaj: brown to gray, calcareous, feature-forming sandstone, and low weathering, gypsum-veined, red marl, and siltstone; Qft2: low-level piedmont fan, and valley terrace deposits)

long time, which the heterogeneity of the reservoir rocks might change during the model calculation, and lead to error in calculation (Huang et al. 2017; Skalinski and Kenter 2015; Yin et al. 2009). Some researchers (Labourdette et al. 2008; Yan-lin et al. 2011) imply a series of basic steps for constructing a 3D reservoir model, and these trials and errors have advanced our knowledge. The key to solving this problem is to build a reasonable 3D spatial data model, develop an efficient modeling method, and develop a user-friendly model operation algorithm. Therefore, engineers found necessity of more efficient and economical techniques to develop and manage complex giant oilfields. Moreover, accurate handling of the uncertainties associated with the various modeling parameters and their integration into the 3D model can provide an estimation of a reliable range of the volume of hydrocarbon in place (Al-Attar 2004; Al-Kadem et al. 2018).

Optimum reservoir characterization and management by 3D modeling need initial data such as well-logs, core samples, well test, and production data (Arnold et al. 2019; Ibrahim et al. 2018). The outputs give valuable and practical information about the volume of space, grain size, thickness, porosity, and formations' permeability. Also, it can recognize the faces in different sedimentary environments (Soleimani et al. 2019; Xuequn et al. 2019).

The geological modeling of the reservoir needs a 3D structure to calculate in-place fluid volumes (Benetatos and Giglio 2019), which has two parts: (i) structural modeling (stratigraphic and fault models) which plays a significant role in the

compartment of a reservoir and often provide the first-order controls on in-place fluid volumes and fluid movement during production. Thus, it is crucial to model the structural frameworks as accurately as possible. (ii) modeling of reservoir features (faces and petrophysical properties) (Balestra et al. 2019; Wu et al. 2006) which describes the structure, stratigraphy, and rock properties of the reservoir and is a powerful tool in geostatistical studies (Chambers et al. 2000; Jin et al. 2020) and geological modeling (Mitra and Leslie 2003; Pan et al. 2020). It can investigate point distance, heterogeneity, spatial variation, and data association (Zamora Valcarce et al. 2006); 3D geo-model grid, water saturation, porosity, and permeability distribution map are made (Nikravesht et al. 1999; Soleimani and Shokri 2015). Besides, one of the primary responsibilities of 3D geological modeling is the structural reconstruction and estimation parameters to calculate oil volume in place, exploitation of oil, and finding the new wells' location (Larue and Friedmann 2005; Pringle et al. 2010).

Zagros fold is one of the significant oil reservoirs in Iran, rich in hydrocarbon reservoirs (Kobraei et al. 2019; Lasemi and Jalilian 2010). This potential has been formed by a combination of flexure slip and natural surface folding mechanism among Zagros oilfields (Bordenave and Hegre 2010; Dehghanzadeh and Adabi 2020; Hakimi and Najaf 2016; Moradi et al. 2017). Among Zagros oilfield, Maroon oilfield in Asmari formations has the most importance for geologists and drillers due to its oil production capacity and high drilling mud loss (Agin et al. 2018;

Table 1 Lithology of classified layers and sublayers

Layer/sublayer	Thickness (m)	Lithology	Zone symbol
Layer 1	50-75	Dolomite, dolomitic lime	Asm1-1
Sublayer 11	18-20	70% sandstone, and small amounts of lime, dolomite, and thin layers of shale	Asm1-2
Layer 20	60-90	60% dolomite, dolomitic lime, thin layers of shale, and marl	Asm2-1-1
Sublayer 28	12-18	Sandstone, lime, sandy lime, dolomite, and shale	Asm2-1-2
Layer 30	30-60	Lime, dolomite, and thin layers of sand and shale existed.	Asm2-1-3
Sublayer 30.60	18-28	Dolomitized sandstone and thin layers of shale in some parts	Asm2-2
Layer 40	120-130	Lime, dolomitic lime, sandstone, and shale/marl	Asm3-1-1
Sublayer 40.80	17-30	90% lime, and thin layers of shale and sand	Asm3-1-2
Layer 50	65-70	Dense clay, limestone, dark glauconite, and pyrite shales	Asm3-1-3
Sublayer 50.60	38-78	Compacted clay lime	Asm3-2

Zare et al. 2019). The present study attempts to deeply explore Maroon oilfield as a giant reservoir using 3D reservoir modeling to produce structural information, which could be essential for decision-makers. In the present study, the volume of oil-in-place of the reservoir and various zones were estimated, and the best zones for future exploitation were introduced. Regarding similar studies, the present study is the most extensive and highly detailed 3D modeling of the greatest hydrocarbon reservoir in the Middle East, which also statistically revealed the petrophysical parameters' interaction.

Material and methods

Geological position

Zagros geological zone in Iran is extended over Iraq territory in the northwest and in some parts of Oman in the south

direction, which is considered one of the world’s richest hydrocarbon basins (Moradi et al. 2017). Zagros is divided into three zones, including (i) imbricate zone, (ii) Uremiah–Dokhtar magmatic zone, and (iii) Zagros folded and thrust belt (Mehrabi et al. 2021) with an area of about 867 km². The maroon oilfield is one of the largest oilfields in Dezful embayment near Aghajari, Ahvaz, and Koopal oilfields (Fig. 1a). It is located in the southeast of Ahvaz City on the quaternary sediments, including low-level piedmont fan and valley terrace deposits. The field has a northwest-southeast direction in length and a northeastern-southwestern direction in width. Active tectonical movements in the Zagros system during Oligocene resulted in many anticlines that provided colossal hydrocarbon reservoirs (Bordenave and Hegre 2010) (Fig. 1b). Overall, the length and width of the field are about 60 and 7 km, respectively. This surficial face is formed in the early Oligocene and mainly includes limestone, sandstone, and evaporate rocks (Alavi Panah 2004). The Asmari

Fig. 2 Isochore depth map of Asmari reservoir in Maroon oilfield

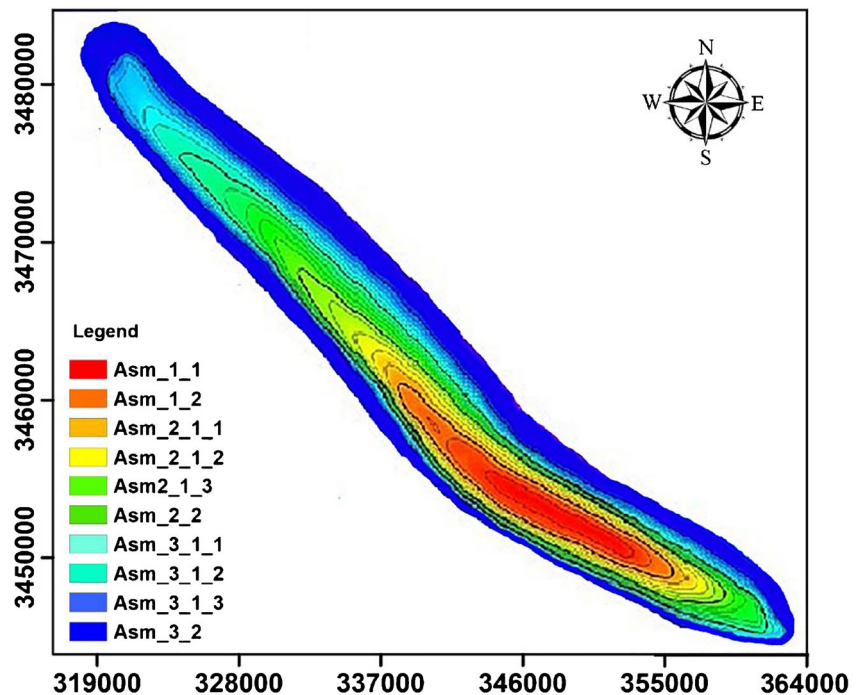
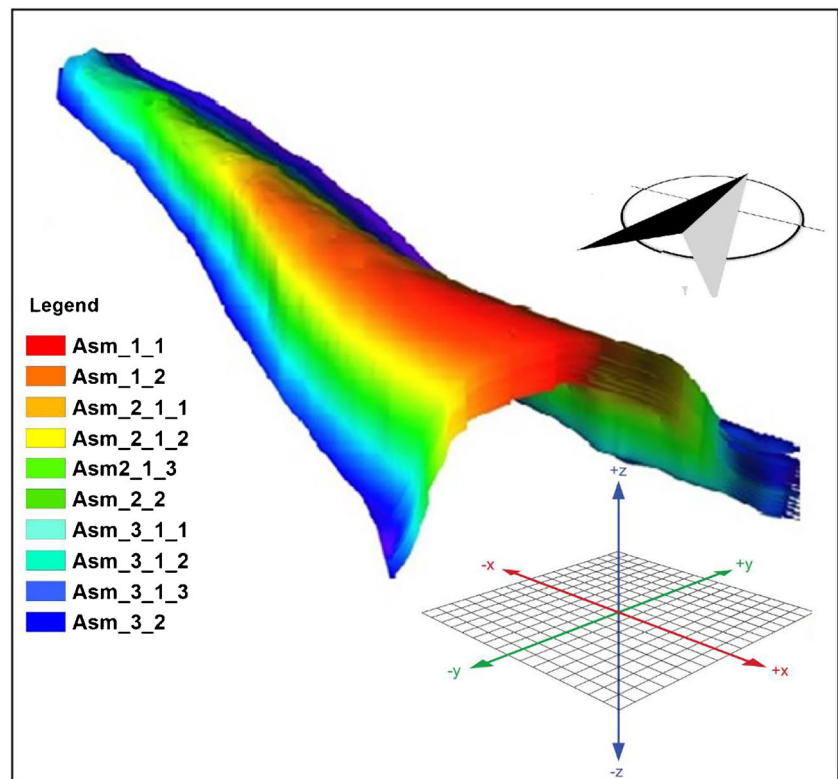


Fig. 3 3D structural modeling of Asmari reservoir in Maroon oilfield



formation, Bangestan formation, and Khami groups constitute this field's oil reservoirs (Jafarzadeh and Hosseini-Barzi 2008).

Modeling and simulation of Asmari formation in Maroon oilfield

Two groups of data were entered into the RMS software to create a static model of the reservoir. First is the number of 86 well data, including geographic coordinates, well deviation, and petrophysical properties. Second, reservoir structural data is involved in calculated horizons based on the underground contour (UGC) map, interpreted horizons, faults, project boundary, contact surfaces of water, oil, and gas (OWC) well-picked. In the following steps, the constructing structural model, 3D model grid, blocked wells, and constructing petrophysical models were simulated. Finally, water saturation ratio, porosity distributions, the ratio of useful thickness to the total thickness or net to growth thickness (NGT), and volumetric calculations were calculated.

Results

Structural modeling

It is necessary to model structural and petrophysical characteristics as an essential framework to simulate the reservoir.

The structural modeling includes modeling of faults, stratigraphic, and 3D geo cellular (grid). In stratigraphic modeling, all the reservoir horizons were calculated based on the interpreted horizons (depth, well deviation), thickness data (isochore), and modeled faults. According to their lithology, the petrophysical properties of interpreted horizons were classified into ten significant layers/sublayers (Table 1).

The isochore depth map of the Asmari reservoir in the Maroon oilfield was plotted by considering each reservoir zone's depth and UGC (Fig. 2). This map shows the opening of the last isochore to the south and possible relation to other structures and implies the possibility of petroleum migration in the past. The 3D stratigraphic model of the Asmari reservoir in the Maroon oilfield was calculated in each oil well and plotted as a structural modeling map (Fig. 3). According to this figure, the field consisted of one culmination related to folding compressing stresses.

The 3D geo cellular model (3D grid) was produced to reveal reservoir heterogeneities in the next step. Gridding is a cell net that other modeling processes are applied to increase data accuracy and improve our understanding of heterogeneity in hydrocarbon reservoirs (Soleimani and Nazari 2012). For this, a net of cells with individual dimensions was defined for the whole reservoir. Therefore, each cell introduces a particular value that can be varied in the order of importance. Controlling the geometry and cell dimensions must be done before giving the weight and run in petrophysical modeling.

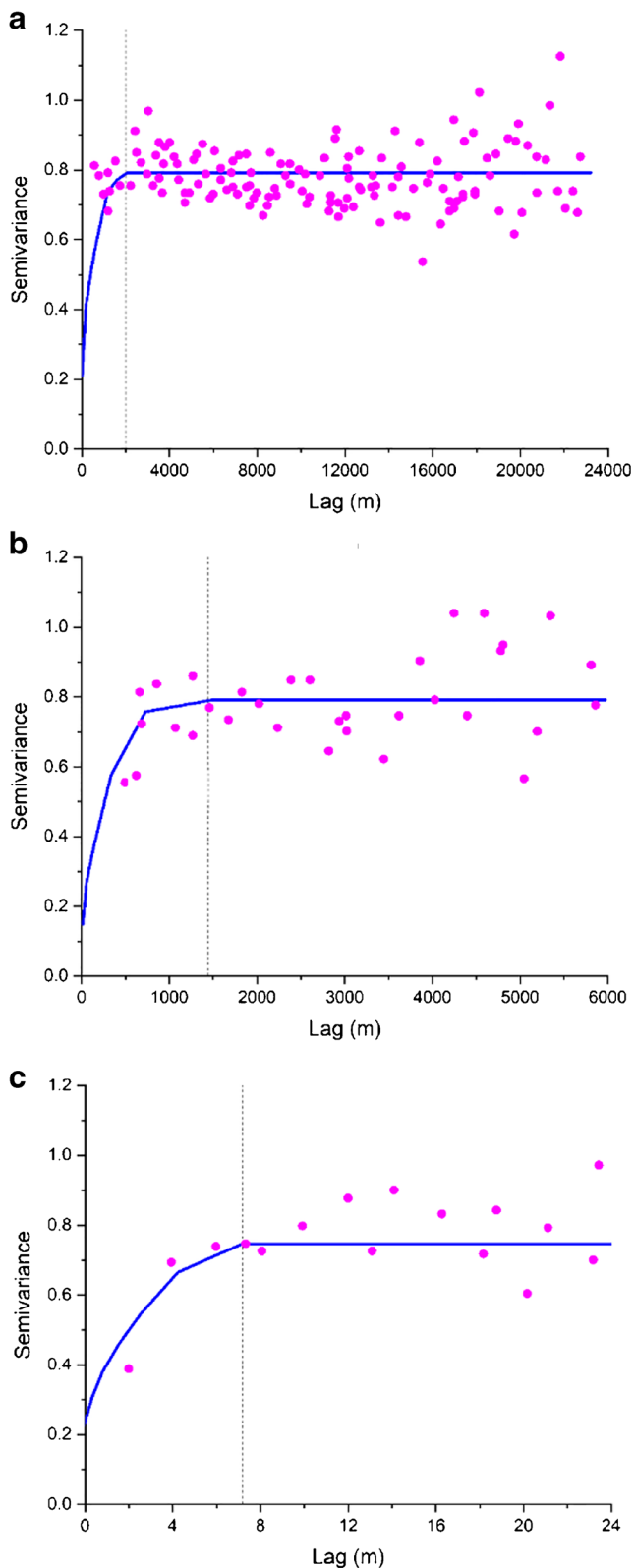


Fig. 4 Variogram calculated by RMS in three directions of **a** X, **b** Y, and **c** Z

The $200 \times 200 \times 1$ m (X.Y.Z) dimensions were selected for each cell to consider the gridding model's space.

Petrophysical modeling

The petrophysical model introduces the estimated distribution of petrophysical properties such as porosity, water saturation, and net to gross thickness. Before running the model, some necessary steps should be done, including rejecting data truncate, except marked trends in the vertical direction, and data transferring to normalize data process. The Asmari reservoir's variogram in the Maroon oilfield was then calculated (Fig. 4) to find the spatial relationship between the data. The figure shows the variability of data corresponding to spatial distance or lag in three directions of X (Fig. 4a), Y (Fig. 4b), and Z (Fig. 4c), which are also mentioned in Fig. 3. Spatial variation remained unchanged for all three graphs at specific lags, which is highlighted with a dot line.

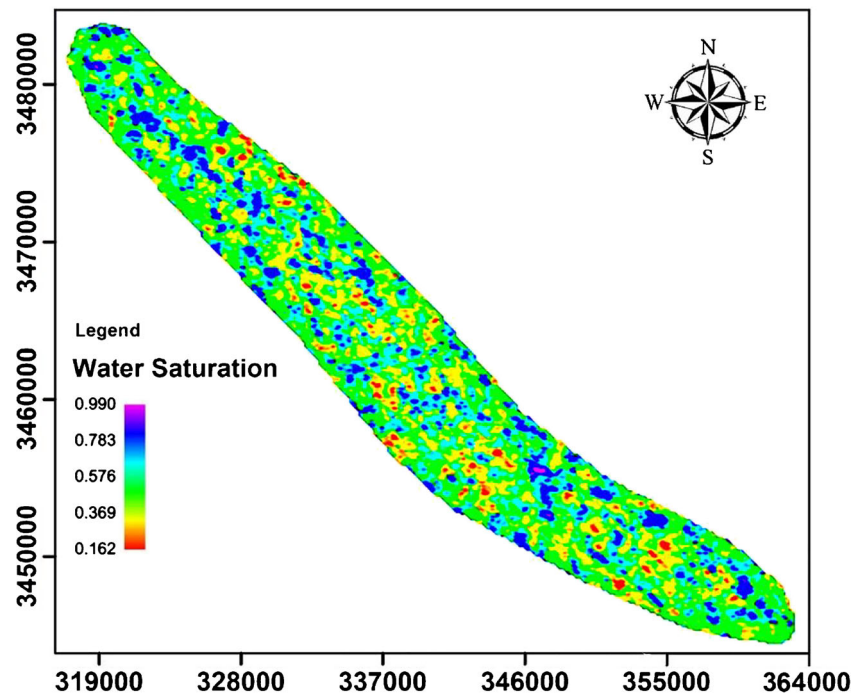
Based on the previous information, some of the most applicable reservoir properties comprising water saturation, porosity, and net to gross thickness were modeled for each zone. The distribution map of the average water saturation percentage for the study area is shown in Fig. 5. As shown in Fig. 5, the saturation ratio is calculated between 0.16 and 0.99. The areas with high saturation ratios are concentrated in the center of the northeast part of the oilfield, and that means there is the least sign of other fluids such as oil and gas, while the great majority of central areas consist of formations with lower water saturation ratios ranges between 0.16 and 0.6. The southern part of the oilfield had an intermediate water saturation condition.

Figure 6 shows the average distribution of porosity ratios in Asmari formation calculated by RMS through well data. As shown, the areas with lower porosity are highlighted with green, yellow, and red colors. Thereby, these areas with clumped dispersion are more susceptible to trap the fluids such as oil. Conversely, it is unlikely that blue colored areas with higher porosity rates are contained oil (Asoodeh and Bagheripour 2013; Gholami and Ansari 2017).

The average NGT ratio distribution map of the Asmari formation is shown in Fig. 7. The ratio is essential to estimate the amount of oil volume in the reservoir (Snyder 1971). Similar to water saturation and porosity maps, NGT has a clumped dispersion pattern. As shown, the blue and purple areas with higher reservoir rocks have NGT between about 0.6 and 1.0, offering potential hydrocarbon resources with up to 40% or higher availability for secondary recovery, while in the other areas with higher non-reservoir rocks, only 15–25% of hydrocarbon can be recovered. One hundred percent recovery is not possible because of residual oil, high oil viscosity, heterogeneity, fractures, and oil-wet rock factors (Worthington 2010).

The estimated petrophysical parameters (water saturation, NGT, and porosity) are shown in Fig. 8a. The radar chart showed that water saturation, porosity, and NGT properties ranged between 31.5–90.00%, 2.70–12.70%, and 2.60–79.00%, respectively. As shown, water saturation stood at

Fig. 5 The distribution map of the average water saturation ratio for Asmari formation in the study area



30% in Am1-1 and reached to 90% in Am2-1-1. After a sharp decrease to 60% in Am2-2, it reached 90% in the lower zones of Am3-1-1 to Am-3-2. NGT was higher in the top zones and began at 55%, and then reached a high of 68% in Am2-1-1. Following a gradual decrease to 23% in Am3-1-1, NGT percentage sharply decreased to a minimum range of 3% in A3-2. The porosity started at nearly 8% in Am1-1 and witnessed a similar

trend with water saturation for the other zones. It peaked at just under 30% in Am2-1-2, and after a fluctuation reached to about 3% in Am3-2.

As shown in Fig. 8b, NGT and porosity have a significant positive correlation of 0.85 while respectively have negative correlations of -0.98 and -0.84 with water saturation. Based on results, hydrocarbon accumulation would increase with increasing porosity of a layer.

Fig. 6 The distribution map of the average porosity for Asmari formation in the study area

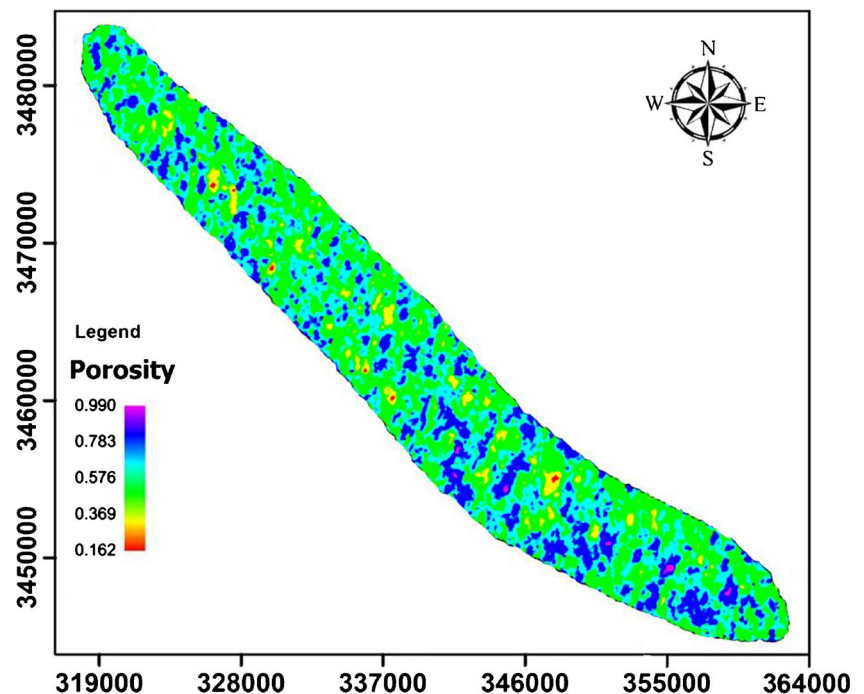
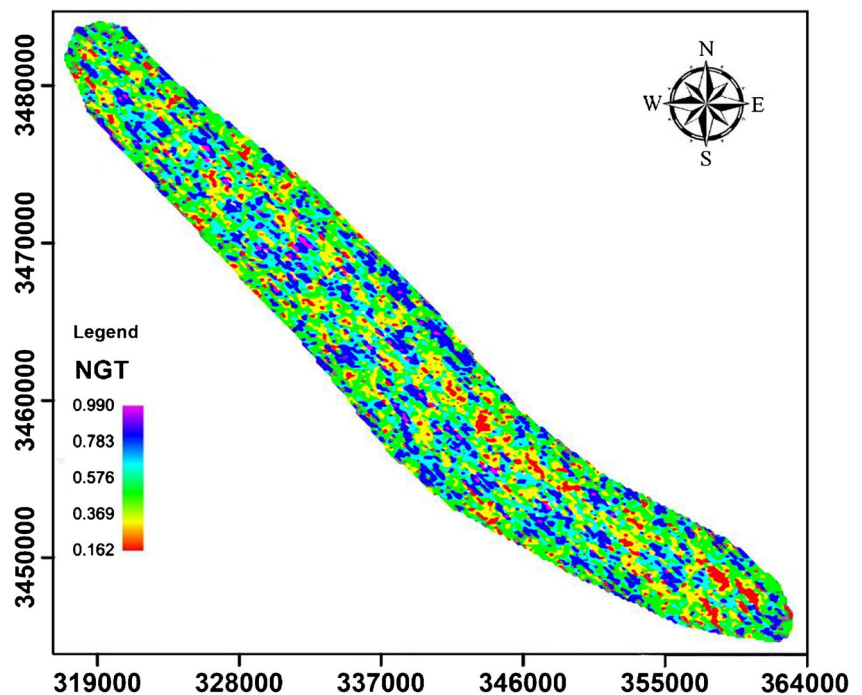


Fig. 7 The distribution map of the average NGT ratio for Asmari formation in the study area



Calculation of the amount of oil volume in place

The precise calculation of original oil-in-place volume is one of the outstanding outputs of 3D simulations of giant oilfields. The amount of volume oil-in-place was estimated by the following equation (Eq. 1):

$$N = \frac{7758A}{B_0} \sum_{i=1}^n h\varphi(1-S_w) \tag{1}$$

where N = oil in place (stb), A = drainage area (acres), B_0 = formation volume factor (rb/stb), h = net pay thickness (ft.), φ = porosity, and S_w = water saturation.

Reserve defines as (Eq. 2):

$$R = N \times E \tag{2}$$

where R = reserves, N = oil in place or free gas reserve, and E = recovery factor.

Based on the above equations, the total and reserve oil volume were 11.5 and 4.4 mm stb, respectively. The amount of oil volume in place for various zones is calculated by Eq. 1 and Eq. 2, shown in Fig. 9a. The pie chart illustrates that the Am2-1-3 and Am1-1 zones possess the highest oil volume percentages of 30.9 and 28.7%, respectively, in the Maroon oilfield. Zones of Am2-1-1 and Am2-2 with 15.3 and 14.2% contained lower oil. The other zones altogether have about 11% of the oil volume of the reservoir. As shown in Fig. 9b, in the zones of Am1-1 to Am2-2, the oil volume has a direct relationship with zone thickness. However, the other underneath zones of Am 3-1-1 to Am3-2, as shown in Fig. 8a, due to water saturation possess lower oil volume.

Discussion

In this research, the geostatistical method was applied as an advanced tool to predict rocks’ performance through geological data. Also, it is known as a powerful tool for understanding data and building spatial distribution models (Hosseini et al. 2019). The 3D geological modeling through drilling, sections, and plane data can provide common platforms for geophysicists, geologists, and engineers to work together (Collon et al. 2015; Philippon et al. 2015). We utilized variogram-based geostatistical techniques to create a 3D model, which is widely applied in the great majority of reservoir-characterization studies (Eidsvik 2015; Pyrcz and Deutsch 2014; Ziegel 2005) because the proper selection of variogram parameters and using adequate data points in the variograms is a key to acquire accurate reservoir characterization (Rossi and Deutsch 2014).

Furthermore, some of the most applicable reservoir parameters comprising water saturation, porosity, and net to gross thickness were modeled for each zone. The average value of the parameters calculated and distributed on the map gave us a general overview of reservoir conditions. The northeast parts of the oilfield had high saturation ratios while the southern part of the oilfield had an intermediate water saturation condition. However, water saturation is not merely representative of fluid distribution because a small proportion of clay minerals and carbonate formation significantly reduces modeling accuracy. Regarding pore size distribution, extensive variations in pore size were observed in carbonate formation. Porosity is a vital parameter for evaluating reservoir formations because the higher porous media store more fluids

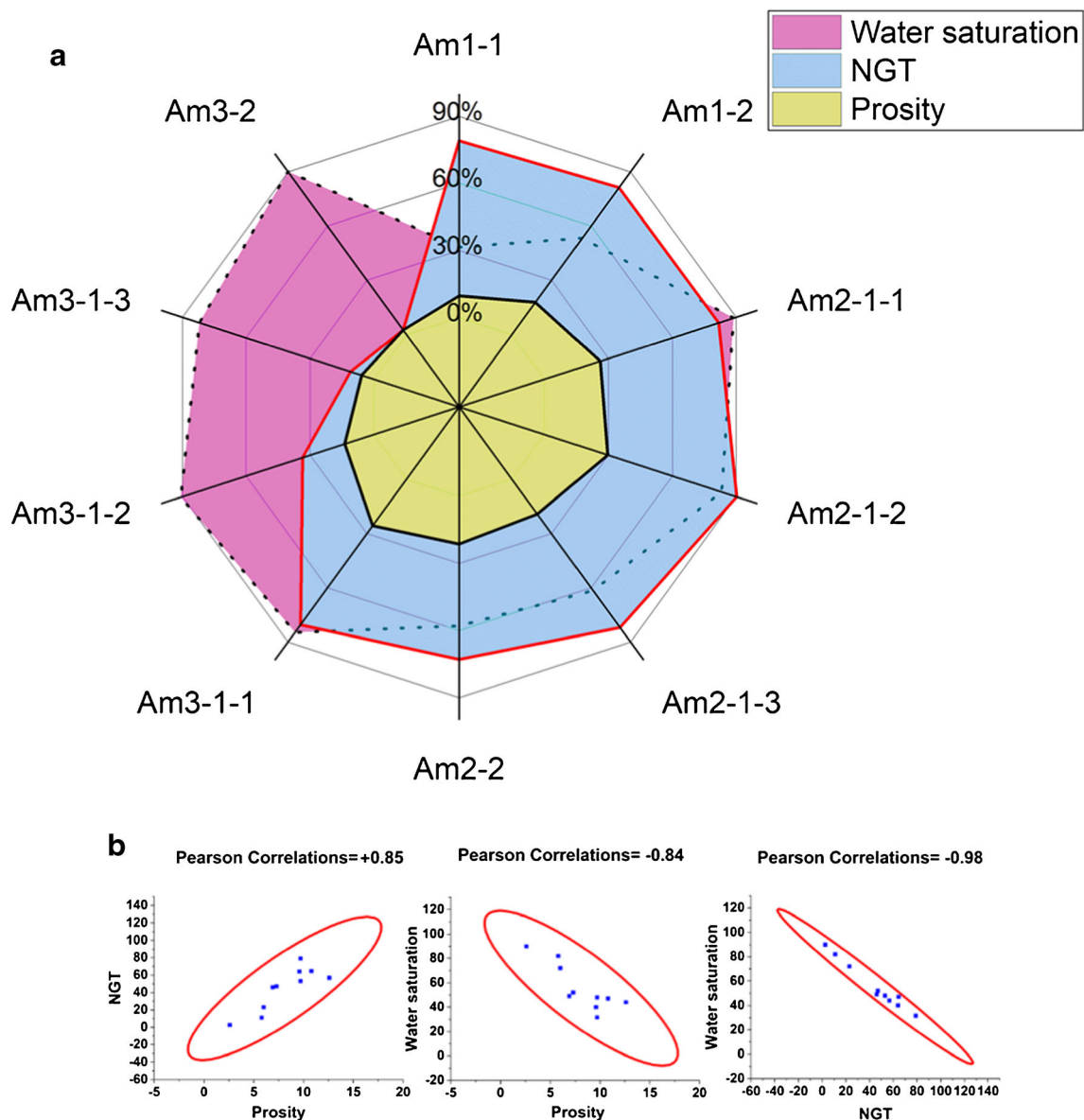


Fig. 8 Illustration of water saturation, NGT, and petrophysical porosity parameters including **a** petrophysical percentages in various zones and **b** Pearson correlation between petrophysical properties

(Alhammedi et al. 2020). Also, the capacity and volume of oil in bedrocks are porosity functions (Pang et al. 2019). However, we should not ignore unrelated connections in rock structures and petrophysical parameters, leading us to different errors during the modeling (Movahhed et al. 2019). Overall, the areas with high porosity values are concentrated in the southern parts, while the areas with high water saturation ratio are approximately located in the northern parts. The porous rocks with a higher NGT ratio are more oil-bearing than those with lower porosity (Metwalli et al. 2018; Xu and Sharif 2020). The converse relation of water saturation with other parameters agrees that the oil-bearing layer has lower water saturation. Therefore, the layers of Am2-1-3, Am2-2, and Am1-1 are seeming to have the highest oil accumulation.

Based on the results, the highest oil-bearing layers consisted of carbonate rocks. Dolomite is the significant component of Asm1-1, Asm1-2, and Asm2-1-1, and shale exists in a thin layer in depth. In contrast, the layers with lower oil volume have other ingredients such as sandstone and clay materials. Sandstone appears from Asm2-1-2 to Asm3-1-1 and is more porous because it is a significant part of Asm3-1-2 and Asm3-1-3, while Asm3-2 mainly consists of a heavy texture component. The compacted clay layers can conversely affect the oil-bearing of geology layers (Lai et al. 2019; Usman et al. 2020; Wooldridge et al. 2017).

This research presented a 3D reservoir model for handling uncertainties in oil reservoirs and provided a reference for future applications and developments. It can help

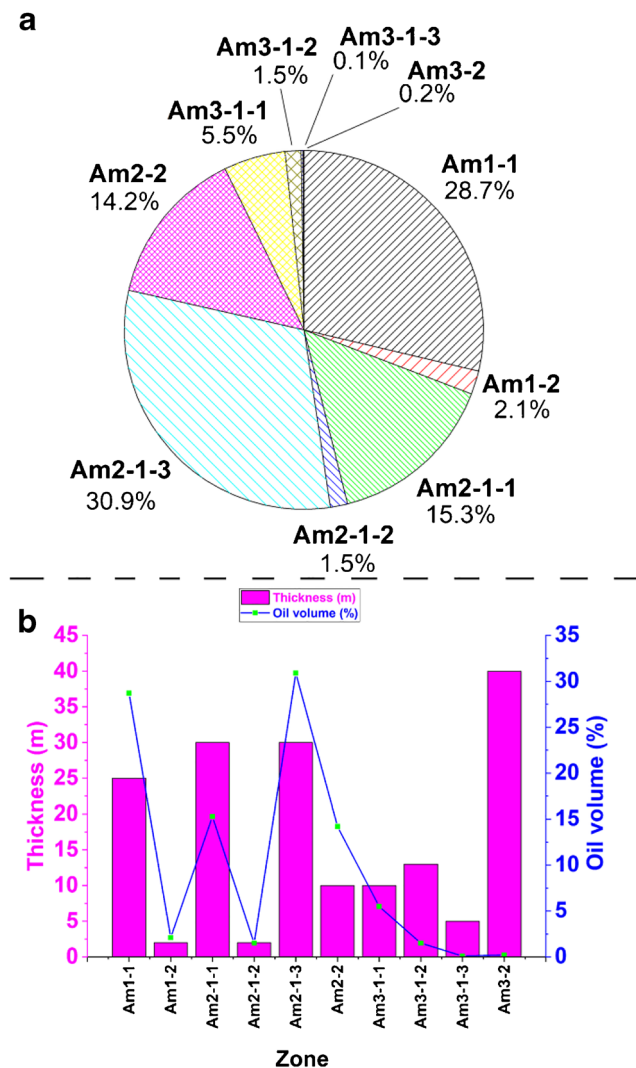


Fig. 9 Graphs of **a** oil volume in place distribution of various zones and **b** thickness of zones, and their calculated oil volume

systematically explore the uncertainty space and estimate the volume of hydrocarbon in place. It was conducted by calculating petrophysical parameters and the volume of oil in place for various layers. The volumetric calculations transferred into separate pie and bar charts allowed the evaluation of each layer's capacity and potential. Knowing the oil-in-place volume for various layers and drawing proper plots for water saturation, porosity and NGT can be a guideline for optimizing future hydrocarbon reservoir development by assessing the level of risks and optimizing investments.

As discussed, the distribution maps of petrophysical properties of water saturation, porosity, and NGT can be a guideline for drilling new wells in the future. Additionally, these platforms have improved data handling and decision-making, leading to more coherent reservoir parameter representation (Philippon et al. 2015; Senel et al. 2014; Xuequn et al. 2019). But one of the critical issues is that the spatial variations of their distribution were severe. For example, the

porosity model showed a slow variation in different directions, and the polygons were more continuous. At the same time, water saturation and NTG modeling showed extreme variation with smaller heterogeneous polygons. Therefore, finding the location of new wells must be done by taking high accurate measures.

Conclusion

- Structural model revealed that the Maroon oilfield is an elongated anticline with a southeast-northwest direction and extends for 60–7 km based on the Asmari formation top.
- The Asmari reservoir in the Maroon oil field is a giant oil field for different reasons, such as low water saturation in most zones and a high oil amount.
- The petrography maps showed that the northwest culmination is the best location for future drilling programs due to low water saturation and NGT.
- The petrophysical properties of porosity and NGT revealed a significant positive correlation with each other and a significant negative correlation with water saturation.
- The first and fifth zones count as the potential petroleum zone as about 60% of the present oil is accumulated there.
- From the seventh to the tenth zone, the oil volume decreased due to high water saturation in these areas.
- The overall method discussed in this research can be applied in various steps during the lifetime of the various reservoirs around the globe.

Declarations

Conflict of interest The authors declare that they have no competing interests.

References

- Aarnes JE (2004) On the use of a mixed multiscale finite element method for greater flexibility and increased speed or improved accuracy in reservoir simulation. *Multiscale Modeling & Simulation* 2:421–439. <https://doi.org/10.1137/030600655>
- Agin F, Khosravanian R, Karimifard M, Jahanshahi A (2018) Application of adaptive neuro-fuzzy inference system and data mining approach to predict lost circulation using DOE technique (case study: Maroon oilfield) *Petroleum*. <https://doi.org/10.1016/j.petlm.2018.07.005>
- Al-Ajmi FA, Holditch SA (2000) Permeability estimation using hydraulic flow units in a central Arabia reservoir. In: *SPE Annual Technical Conference and Exhibition*, SPE-63254-MS.10.2118/63254-MS
- Al-Attar AE (2004) A review of upstream development policies in Kuwait *OPEC Review* 28:275–288. <https://onlinelibrary.wiley.com/doi/abs/10.1111/j.0277-0180.2004.00138.x>

- Alavi Panah S (2004) Study of desertification and land changes of playa Damghan by using Multitemporal and Multispectral Satellites Desert Journal 9:144–154. <https://www.sid.ir/en/journal/ViewPaper.aspx?id=33739>
- Al-Bulushi NI, King PR, Blunt MJ, Kraaijeveld M (2012) Artificial neural networks workflow and its application in the petroleum industry. *Neural Comput & Applic* 21:409–421. <https://doi.org/10.1007/s00521-010-0501-6>
- Alhammadi AM, Gao Y, Akai T, Blunt MJ, Bijeljic B (2020) Pore-scale X-ray imaging with measurement of relative permeability, capillary pressure and oil recovery in a mixed-wet micro-porous carbonate reservoir rock. *Fuel* 268:117018. <https://www.sciencedirect.com/science/article/pii/S0016236120300132>
- Al-Kadem M, Al Yateem K, Al Amri M (2018) Smart oilfield technologies and management: maximizing real-time surveillance and utilization. Paper presented at the SPE Annual Technical Conference and Exhibition, <https://doi.org/10.2118/191493-MS>
- Arnold D, Demyanov V, Rojas T, Christie M (2019) Uncertainty quantification in reservoir prediction: part 1—model realism in history matching using geological prior definitions. *Math Geosci* 51:209–240
- Asoodeh M, Bagheripour P (2013) Core porosity estimation through different training approaches for neural network: back-propagation learning vs. genetic algorithm *International Journal of Computer Applications* 63. <https://doi.org/10.5120/10461-5172>
- Avansi GD, Maschio C, Schiozer DJ (2016) Simultaneous history-matching approach by use of reservoir-characterization and reservoir-simulation studies. *SPE Reserv Eval Eng* 19:694–712. <https://doi.org/10.2118/179740-PA>
- Balestra M, Corrado S, Aldega L, Morticelli MG, Sulli A, Rudkiewicz J-L, Sassi W (2019) Thermal and structural modeling of the Scillato wedge-top basin source-to-sink system: insights into the Sicilian fold-and-thrust belt evolution (Italy). *Bulletin* 131:1763–1782. <https://doi.org/10.1130/B35078.1>
- Benetatos C, Giglio G (2019) Coping with uncertainties through an automated workflow for 3D reservoir modelling of carbonate reservoirs. *Geoscience Frontiers*
- Bordenave M, Hegre J (2010) Current distribution of oil and gas fields in the Zagros Fold Belt of Iran and contiguous offshore as the result of the petroleum systems Geological Society, London, Special Publications 330:291–353. <https://doi.org/10.1016/j.gsf.2019.11.008>
- Chambers RL, Yarus JM, Hird KB (2000) Petroleum geostatistics for nongeostatisticians: part 1. *Lead Edge* 19:474–479. <https://doi.org/10.1190/1.1438630>
- Chen Y, Durlofsky LJ (2006) Adaptive local–global upscaling for general flow scenarios in heterogeneous formations. *Transp Porous Media* 62:157–185. <https://doi.org/10.1007/s11242-005-0619-7>
- Christoforos B, Dario V (2010) Fully integrated hydrocarbon reservoir studies: myth or reality? *American Journal of Applied Sciences* 7. <https://thescpub.com/abstract/ajassp.2010.1477.1486>
- Collon P, Steckiewicz-Laurent W, Pellerin J, Laurent G, Caumon G, Reichart G, Vaute L (2015) 3D geomodelling combining implicit surfaces and Voronoi-based remeshing: a case study in the Lorraine Coal Basin (France). *Comput Geosci* 77:29–43. <https://www.sciencedirect.com/science/article/pii/S0098300415000102>
- Dehghanzadeh M, Adabi MH (2020) Petrography of carbonate rocks in the Asmari Formation, Zagros Basin, Dezful Embayment and Izeh Zone, SW Iran. *Arab J Geosci* 13:1–15. <https://doi.org/10.1007/s12517-020-05855-0>
- Eidsvik J (2015) Pyrcz and Deutsch: geostatistical reservoir modeling. *Math Geosci* 47:497–499. <https://doi.org/10.1007/s11004-015-9588-8>
- Elkatatny S, Mahmoud M, Tariq Z, Abdulaheem A (2018) New insights into the prediction of heterogeneous carbonate reservoir permeability from well logs using artificial intelligence network. *Neural Comput & Applic* 30:2673–2683. <https://doi.org/10.1007/s00521-017-2850-x>
- Gholami A, Ansari HR (2017) Estimation of porosity from seismic attributes using a committee model with bat-inspired optimization algorithm. *J Pet Sci Eng* 152:238–249. <https://doi.org/10.1016/j.petrol.2017.03.013>
- Hakimi MH, Najaf AA (2016) Origin of crude oils from oilfields in the Zagros Fold Belt, southern Iraq: relation to organic matter input and paleoenvironmental conditions. *Mar Pet Geol* 78:547–561. <https://doi.org/10.1016/j.marpetgeo.2016.10.012>
- Hosseini E, Gholami R, Hajjivand F (2019) Geostatistical modeling and spatial distribution analysis of porosity and permeability in the Shurijeh-B reservoir of Khangiran gas field in Iran. *J Pet Explor Prod Technol* 9:1051–1073. <https://doi.org/10.1007/s13202-018-0587-4>
- Huang Z, Liu G, Li T, Li Y, Yin Y, Wang L (2017) Characterization and control of mesopore structural heterogeneity for low thermal maturity shale: a case study of Yanchang Formation Shale. *Ordos Basin Energy Fuels* 31:11569–11586. <https://doi.org/10.1021/acs.energyfuels.7b01414>
- Ibrahim MM, Abdulaziz AM, Fattah KA (2018) STOIP validation for a heterogeneous multi-layered reservoir of a mature field using an integrated 3D geo-cellular dynamic model. *Egypt J Pet* 27:887–896. <https://doi.org/10.1016/j.ejpe.2018.01.004>
- Jafarzadeh M, Hosseini-Barzi M (2008) Petrography and geochemistry of Ahwaz Sandstone Member of Asmari Formation, Zagros, Iran. Implications on provenance and tectonic setting *Revista mexicana de ciencias geológicas* 25:247–260 http://www.scielo.org.mx/scielo.php?script=sci_arttext&pid=S1026-87742008000200005&nrm=iso
- Jin X, Wang G, Tang P, Hu C, Liu Y, Zhang S (2020) 3D geological modelling and uncertainty analysis for 3D targeting in Shanggong gold deposit (China). *J Geochem Explor* 210:106442. <https://doi.org/10.1016/j.gexplo.2019.106442>
- Kobraei M, Sadouni J, Rabbani AR (2019) Organic geochemical characteristics of Jurassic petroleum system in Abadan Plain and north Dezful zones of the Zagros basin, southwest Iran. *Journal of Earth System Science* 128:50. <https://doi.org/10.1007/s12040-019-1082-0>
- Labourdette R, Hegre J, Imbert P, Insalaco E (2008) Reservoir-scale 3D sedimentary modelling: approaches to integrate sedimentology into a reservoir characterization workflow Geological Society, London, Special Publications 309:75–85. <https://sp.lyellcollection.org/content/specpubgsl/309/1/75.full.pdf>
- Lai J et al (2019) Origin and formation mechanisms of low oil saturation reservoirs in Nanpu Sag, Bohai Bay Basin. *China Marine and Petroleum Geology* 110:317–334. <https://www.sciencedirect.com/science/article/pii/S0264817219303319>
- Larue D, Friedmann F (2005) The controversy concerning stratigraphic architecture of channelized reservoirs and recovery by waterflooding. *Pet Geosci* 11:131–146. <https://doi.org/10.1144/1354-079304-626>
- Lasemi Y, Jalilian A (2010) The Middle Jurassic basinal deposits of the Sumeh Formation in the Central Zagros Mountains, southwest Iran: facies, sequence stratigraphy, and controls. *Carbonates Evaporites* 25:283–295. <https://doi.org/10.1007/s13146-010-0032-3>
- Le Ravalec M, Doligez B, Lerat O (2014) Integrated reservoir characterization and modeling IFPEN E-book. <https://doi.org/10.2516/ifpen/2014001>
- Mehrabi H, Bahrehvar M, Rahimpour-Bonab H (2021) Porosity evolution in sequence stratigraphic framework: a case from Cretaceous carbonate reservoir in the Persian Gulf, southern Iran *Journal of Petroleum Science and Engineering* 196:107699. <http://www.sciencedirect.com/science/article/pii/S0920410520307646>
- Metwalli FI, Pigott JD, Ramadan FS, El-Khadragy AA, Afify WA (2018) Alam El Bueib reservoir characterization, Tut oil field, North

- Western Desert. *Egypt Environmental Earth Sciences* 77:143. <https://doi.org/10.1007/s12665-018-7290-0>
- Mitra S, Leslie W (2003) Three-dimensional structural model of the Rhourde el Baguel field. *Algeria AAPG bulletin* 87:231–250. <https://doi.org/10.1306/07120201114>
- Moradi M, Moussavi-Harami R, Mahboubi A, Khanebad M, Ghabeishavi A (2017) Rock typing using geological and petrophysical data in the Asmari reservoir, Aghajari Oilfield, SW Iran. *J Pet Sci Eng* 152:523–537. <https://doi.org/10.1016/j.petrol.2017.01.050>
- Movahhed A, Bidhendi MN, Masihi M, Emamzadeh A (2019) Introducing a method for calculating water saturation in a carbonate gas reservoir. *Journal of Natural Gas Science and Engineering* 70: 102942. <https://doi.org/10.1016/j.jngse.2019.102942>
- Nikravesh M, Zadeh LA (2007) Forging new frontiers: fuzzy pioneers I vol 217. *Studies in Fuzziness and Soft Computing*. Springer-Verlag, Berlin Heidelberg. <https://doi.org/10.1007/978-3-540-73182-5>
- Nikravesh M, Levey RA, Adams RD, Ekart D (1999) Soft computing: tools for intelligent reservoir characterization (IRESC). In: SEG Technical Program Expanded Abstracts 1999. Society of Exploration Geophysicists, pp 977–980. 10.1190/1.1821276
- Pan D, Xu Z, Lu X, Zhou L, Li H (2020) 3D scene and geological modeling using integrated multi-source spatial data: methodology, challenges, and suggestions *Tunnelling and Underground Space Technology* 100:103393. 10.1016/j.tust.2020.103393
- Pang H, Ding X, Pang X, Geng H (2019) Lower limits of petrophysical parameters allowing tight oil accumulation in the Lucaogou Formation, Jimusaer Depression, Junggar Basin, Western China *Marine and Petroleum Geology* 101:428–439 <https://www.sciencedirect.com/science/article/pii/S0264817218305518>
- Philippon M, Le Carlier de Veslud C, Gueydan F, Brun J-P, Caumon G (2015) 3D geometrical modelling of post-foliation deformations in metamorphic terrains (Syros, Cyclades, Greece). *J Struct Geol* 78: 134–148 <https://www.sciencedirect.com/science/article/pii/S0191814115300110>
- Pouladi B, Sharifi M, Ahmadi M, Kelkar M (2017) Fast marching method assisted sector modeling: application to simulation of giant reservoir models. *J Pet Sci Eng* 149:707–719. <https://doi.org/10.1016/j.petrol.2016.11.011>
- Pringle JK, Brunt RL, Hodgson DM, Flint S (2010) Capturing stratigraphic and sedimentological complexity from submarine channel complex outcrops to digital 3D models, Karoo Basin, South Africa. <https://doi.org/10.1144/1354-079309-028>
- Pyrcz MJ, Deutsch CV (2014) *Geostatistical reservoir modeling*. Oxford university press.
- Rossi ME, Deutsch CV (2014) Data collection and handling *Mineral Resource Estimation*:67–96. https://doi.org/10.1007/978-1-4020-5717-5_5
- Senel O, Will R, Butsch RJ (2014) Integrated reservoir modeling at the Illinois Basin–Decatur project. *Greenhouse Gases: Science and Technology* 4:662–684. <https://doi.org/10.1002/ghg.1451>
- Skalinski M, Kenter JA (2015) Carbonate petrophysical rock typing: integrating geological attributes and petrophysical properties while linking with dynamic behaviour *Geological Society, London, Special Publications* 406:229–259. <https://doi.org/10.1144/SP406.6>
- Snyder RH (1971) A review of the concepts and methodology of determining “net pay”. In: Fall Meeting of the Society of Petroleum Engineers of AIME, Society of Petroleum Engineers. 10.2118/3609-MS
- Soleimani B, Nazari F (2012) Petroleum reservoir simulation, Ramin Oil Field, Zagros, Iran. *International Journal of Modeling and Optimization* 2:672. <https://doi.org/10.7763/IJMO.2012.V2.207>
- Soleimani M, Shokri BJ (2015) 3D static reservoir modeling by geostatistical techniques used for reservoir characterization and data integration. *Environ Earth Sci* 74:1403–1414. <https://doi.org/10.1007/s12665-015-4130-3>
- Soleimani B, Moradi M, Ghabeishavi A, Mousavi A (2019) Permeability variation modeling and reservoir heterogeneity of Bangestan carbonate sequence, Mansouri oilfield, SW Iran. *Carbonates Evaporites* 34:143–157. <https://doi.org/10.1007/s13146-018-0461-y>
- Usman M et al. (2020) Linking the influence of diagenetic properties and clay texture on reservoir quality in sandstones from NW Borneo *Marine and Petroleum Geology* 120:104509. <https://www.sciencedirect.com/science/article/pii/S0264817220302920>
- Woolridge LJ, Worden RH, Griffiths J, Utley JE (2017) Clay-coated sand grains in petroleum reservoirs: understanding their distribution via a modern analogue. *J Sediment Res* 87:338–352. <https://doi.org/10.2110/jsr.2017.20>
- Worthington PF (2010) Net pay-what is it? What does it do? How do we quantify it? How do we use it? *SPE Reserv Eval Eng* 13:812–822. <https://doi.org/10.2118/123561-PA>
- Wu K et al (2006) 3D stochastic modelling of heterogeneous porous media—applications to reservoir rocks. *Transp Porous Media* 65: 443–467. <https://doi.org/10.1007/s11242-006-0006-z>
- Xu C, Sharif AH (2020) Untangle shale and gas effects to estimate porosity and net/gross ratio using a boomerang workflow—a case study in shoreface reservoirs in Brunei *Petrophysics* 61:112–127. 10.30632/PJV61N1-2020a5
- Xuequn T, Yunyan L, Xiaozhou Z, Jiandang L, ZHENG R, Chao J (2019) Multi-parameter quantitative assessment of 3D geological models for complex fault-block oil reservoirs. *Pet Explor Dev* 46: 194–204. [https://doi.org/10.1016/S1876-3804\(19\)30019-9](https://doi.org/10.1016/S1876-3804(19)30019-9)
- Yan-lin S, Ai-ling Z, You-bin H, Ke-yan X (2011) 3D geological modeling and its application under complex geological conditions. *Procedia Engineering* 12:41–46 <https://www.sciencedirect.com/science/article/pii/S1877705811009222>
- Yin S, Dusseault MB, Rothenburg L (2009) Thermal reservoir modeling in petroleum geomechanics. *Int J Numer Anal Methods Geomech* 33:449–485. <https://doi.org/10.1002/nag.723>
- Zamora Valcarce G, Zapata T, Ansa A, Selva G (2006) Three-dimensional structural modeling and its application for development of the El Portón field. *Argentina AAPG bulletin* 90:307–319. <https://doi.org/10.1306/09300504142>
- Zare N, Bonakdarpour B, Amoozegar MA, Shavandi M, Fallah N, Darabi S, Taromsary NB (2019) Using enriched water and soil-based indigenous halophilic consortia of an oilfield for the biological removal of organic pollutants in hypersaline produced water generated in the same oilfield. *Process Saf Environ Prot* 127:151–161. <https://doi.org/10.1016/j.psep.2019.04.024>
- Zhi Y, Caineng Z (2019) “Exploring petroleum inside source kitchen”: connotation and prospects of source rock oil and gas. *Pet Explor Dev* 46:181–193. [https://doi.org/10.1016/S1876-3804\(19\)30018-7](https://doi.org/10.1016/S1876-3804(19)30018-7)
- Ziegel E (2005) Geostatistical reservoir modeling. *Technometrics* 47: 527–527. <https://doi.org/10.1198/tech.2005.s339>